Jurnal Praktik
Keinsinyuran
e-ISSN:3063-7449

Jurnal **Praktik Keinsinyuran** Vol.2 No.5 (November 2025)
journal homepage: http://ejournal.atmajaya.ac.id/index.php/jpk

Root Caused Failure Analysis Deodorizer Column at Expansion Bellow and Vacuum Chamber Connection to Column in Refinery Plant

Muhammad Adyutatama[1,2*], Hadi Sutanto[3]

[1]Program Studi Program Profesi Insinyur, Fakultas Biosains, Teknologi, dan Inovasi, Universitas Katolik Indonesia Atma Jaya, Jalan Jenderal Sudirman 51 Jakarta 12930

[2]Program Studi Magister Teknik Mesin, Fakultas Biosains, Teknologi, dan Inovasi, Universitas Katolik Indonesia Atma Jaya, Jalan Jenderal Sudirman 51 Jakarta 12930

[3]Program Studi Teknik Mesin, Fakultas Biosains, Teknologi, dan Inovasi, Universitas Katolik Indonesia Atma Jaya, Jalan Jenderal Sudirman 51 Jakarta 12930

Article Info

Article history:

Received
July, 18 2025

Accepted
July, 22 2025

Keywords: Root Caused Failure Analysis, Vacuum Chamber, Fatigue.

Abstract

Vacuum chamber that connecting the deodorizer column to the condenser had collapsed. The leaks were potentially occurring prior to the collapse of the vacuum chamber. The loading and unloading operation could make a fluctuating dynamic stress. In addition to the fluctuating dynamic stresses, fatigue failure mechanism had occured. The crack developed and gradually propagated in the welded joints which welded on the site due to it was proved have low mechanical properties as shown in tensile test. Follow the welding procedure specification (WPS) document, inspect the preparation of the welding process to ensure that the single-V groove is being prepared appropriately, inspect the weld during and/or after the welding process to ensure that it has achieved complete joint penetration and employ another non-destructive testing method, such as radiography, to verify the completeness of the joint penetration are recommended to prevent the similar failure in the future.

Info Artikel

Histori Artikel:

Diserahkan:
18 Juli 2025

Diterima:
22 Juli 2025

Kata Kunci: Analisa Kegagalan, *Vacuum Chamber*, Fatik.

Abstrak

Vacuum chamber yang berfungsi menghubungkan kolom deodorisasi dengan kondensor mengalami kegagalan. Indikasi menunjukkan bahwa kebocoran telah terjadi sebelum terjadinya kegagalan tersebut. Aktivitas operasi terkait masuk dan keluarnya fluida diperkirakan menghasilkan tegangan dinamis yang berfluktuasi, yang selanjutnya berkontribusi terhadap inisiasi dan propagasi retak. Selain pengaruh tegangan dinamis, mekanisme kegagalan fatik juga ikut berperan. Retak berkembang dan merambat secara gradual pada sambungan las yang dilakukan di lapangan, yang menunjukkan sifat mekanik rendah berdasarkan hasil uji tarik. Berdasarkan dokumen *Welding Procedure Specification* (WPS), beberapa tindakan mitigasi direkomendasikan untuk mencegah kegagalan serupa. Tindakan tersebut meliputi verifikasi kesiapan proses pengelasan guna memastikan bahwa *single-V groove* dipersiapkan secara memadai, pemeriksaan kualitas las selama dan/atau setelah proses pengelasan untuk memastikan terwujudnya penetrasi sambungan lasan yang baik, serta penerapan metode pengujian non-destruktif tambahan, seperti radiografi, untuk memvalidasi pencapaian penetrasi sambungan lasan secara menyeluruh.

*Corresponding author. Muhammad Adyutatama
Email address: adyutatama@gmail.com

1. INTRODUCTION

It was discovered that the vacuum chamber that connecting the condenser to the deodorizer tray had collapsed. This vacuum chamber materials is 304 stainless steel which commonly used. Stainless steel has outstanding corrosion resistance, an elegant surface effect, and good mechanical properties (Yang Peng, Jie Chen, Jun Dong., 2019). This deodorizer had been operated for two years period. Prior to the incident, there was an anomaly in the pressure level a few hours beforehand. The leaks were potentially occurring prior to the collapse of the vacuum chamber. Following the collapse, the whole production process was immediately stopped. The root caused failure analysis (RCFA) team scheduled a visit to the Refinery Plant for the purpose of conducting a visual inspection and collecting samples for further analysis. The horizontal vacuum chamber was equipped with the expansion bellow structures (e.g. consist of 2 wavy plates), which served the aim of minimizing thermal expansion throughout the production process. The expansion structures also failed structurally. Furthermore, tear in the weld joints were found on the curved region (between horizontal and vertical vacuum chamber). On the other hand, the collapse of the vertical vacuum chamber happened at the welded area, with no sign of failure or leakage starting on the material side. This technical study was developed to analyse the underlying cause of the failure and implement measures to prevent a similar risk in the future.

2. RESEARCH METHODS

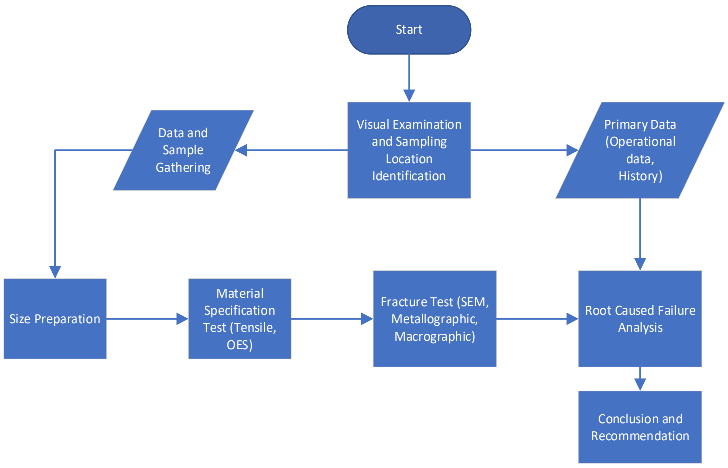

Figure 1.
Methodology of Root Caused Failure Analysis

The investigation starts with visual inspection in the refinery plant to collect data sample and investigate the chronology of the failure:

a. Horizontal Vacuum Chamber

The failures result in the complete collapse of the condenser-to-deodorizer vacuum chamber. Subsequently, we attempted to locate the specific regions of failure within the whole vacuum chambers. The regions of failure included the expansion structures, tears in the weld joints of the curved structures (between the horizontal and vertical vacuum chamber), and tears in the weld joints of the vertical vacuum chamber. Figure 2 illustrates the occurrence of collapsed structures at the horizontal vacuum chamber, which connected the ice-condenser on the left side to the vertical vacuum chamber on the right side. The whole structures were compressed, indicating their inability to sustain the vacuum pressure at that moment. Moreover, the investigation extended to the regions where failures occurred in the expansion structures. The failures indicated that plastic deformation had taken place on both the right and left sides of the expansion structures. The welded joints on the expansion structures remained intact, suggesting that the failures were not related with the joint in the expansion structure. In order to determine the cause of the failures, samples of the expansion structures were gathered and examined using scanning electron microscopy (SEM).

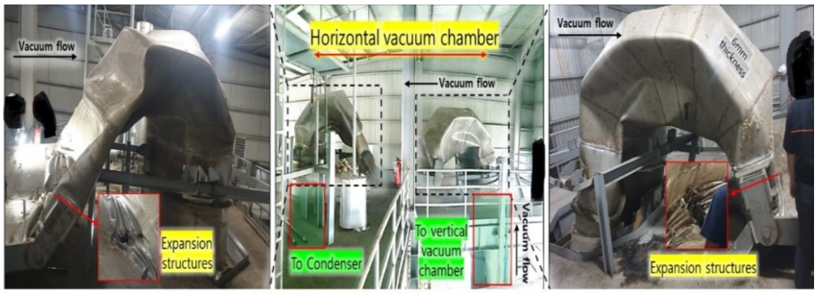

Figure 2.
The Failures of Expansion Structures at Horizontal Vacuum Chamber

Inside the horizontal vacuum chamber, black soot was found along with water mixed with oil. However, based on field information, the presence of this water is likely due to the cooling process that followed a fire incident. The presence of a fluid with an oily consistency suggests the possibility of residual fatty acids being carried into this area. In general, from external observations, no significant thinning was detected. Additionally, upon visual inspection of the tear area on the expansion joint after it was cut, no thinning was observed. The absence of the thinning indicates the general corrosion attack did not happen in this incident. Figure 3 represents failure area in the horizontal vacuum chamber, specifically highlighting crack and tear in the welded joints and other unusual findings. This area is located at the curving section that connected the horizontal and vertical vacuum chambers. The failures in this image are shown in the welded joints, particularly in the areas where there was a noticeable white colour difference near the welded joints. The white colour difference observed in welded joints was a result of the inspection conducted using a non-destructive testing method (e.g. penetrant test). Contrary to another welding line, the failures exclusively occurred in this welding line that had a white colour contrast. It suggests that the mechanical quality of the welding with white colour contrast was lower to that of other welded joints. Upon further investigation, it was found that the white colour contrast welding line originated from the welding process conducted on-site at the Refinery Plant and the other welded joints were a result of the welding process carried out at the fabrication company.

Figure 3.
The Failures at Horizontal Vacuum Chamber (cont.)

Additional unusual observations were noticed on the welded joints that were welded on-site. These included the presence of an uneven pattern of welding reinforcements on the joint surface, namely a 1-cap (or 1 welding line) and a 3-cap (3 welding line) as seen in Figure 3. The failures happened in the 1-cap welding line. According to this evidence, it has been verified that the tears in the welded joints originated from the low tensile properties of the 1-cap welding line, rather than the 3-cap welding line. Furthermore, these unusual welding reinforcements (1-cap and 3-cap) originated from the different weld joint designs. Two chamber plates were welded using 1-cap welding reinforcement. Alternatively, a 3-cap welding reinforcement involved the welding of two chamber plates with a third plate sandwiched in between. The findings indicated that the welders implemented additional precautions, perhaps in response to mitigating the significant distortion that occurs during the welding process. Unfortunately, those actions had an impact on the variation in mechanical characteristics along the welding line. During the operation, when the loading occurs in this welded line, the stress tolerance of the welding line varies. In this circumstance, the 1-cap welding line is more prone to failure, and it confirmed by the failure location.

b. Vertical Vacuum Chamber

A vertical vacuum chamber serves as a conduit that connects the horizontal vacuum chamber to the deodorizer tray. As illustrated in Figure 4, failures predominantly occurred at the weld joints which connecting the 6mm thick plate to the 12 mm thick chamber plate. This type of failure mirrors the defects observed at the curved section of the horizontal vacuum chamber, where the weld joints were completed on-site. Upon closer inspection at higher magnification, tears in the welded joints were evident, along with the propagation of cracks originating from the weld region. Despite these observations, no signs of leakage were detected in either the 6mm or 12 mm thick material. The failures further suggest that the 6mm thick chamber plate experiences movement and compression against the adjacent plate following the weldment failure.

Figure 4.
The Failures at Vertical Vacuum Chamber

The fracture surface analysis of the failed welded joints, with thicknesses of 6mm and 12 mm, revealed that improper welding techniques were employed throughout the process. Initially, the welding penetration depth was limited to approximately 2-3 mm, whereas the welding process specification (WPS) document prescribed a penetration depth of 6mm. Additionally, the presence of a 3mm flat section, resulting from the 6mm thick chamber plate, indicates that the single-V groove specified in the WPS document was not adequately formed during the welding preparation process. These observations suggest that it was challenging for the welders to achieve complete joint penetration at the time. Furthermore, the criteria for pressure vessel applications, as outlined in the American Society of Mechanical Engineers (ASME) Section IX code, are insufficient for cases of partial penetration. These criteria include the use of radiography (QW-191.1.2) and ultrasonic tests (QW-191.2.2) (American Society of Mechanical Engineers, 2023). However, the on-site inspection of the welding was limited to a dye-penetrant test, which only detects surface crack indications. Similar to the horizontal vacuum chamber section, a black deposit is found inside the vacuum chamber. No significant general thinning was found at the external side and also no significant thinning found from the failure area near the welding.

c. Pressure Level Monitoring Before the Failures

Based on the visual investigation of the failures mentioned earlier in the connection vacuum chamber between the ice-condenser and deodorizer, three specific locations were identified where the failures occurred. These locations include the expansion structures, the welded joint at the curved region of the horizontal vacuum chamber, and the welded joint at the vertical vacuum chamber. Hence, conducting an in-depth investigation into the prior activities leading up to the accident is crucial in order to comprehend what happened before the occurrence of the failures. Figure 5. displays the monitoring of pressure levels a few hours before to the failure, together with the corresponding condition state within a certain time period. Starting from the evening of May 27th, the pressure level remained at a normal condition. Furthermore, there was an action taken to replace the pump at around 19:00. Subsequently, the refinery is brought to the initial operating state by gradually reducing the pressure level until it reaches a vacuum condition. After determining the operational pressure level range, the feeding condition commenced at around 22:00. Unfortunately, a deviation in the monitoring of pressure levels was detected at around 23:00. The pressure level exhibited a consistent change with a progressive increase. The flushing is a corrective treatment performed by operators to regulate the pressure level and return it to the acceptable range for operational conditions. According to the findings from monitoring the pressure levels, there is a significant possibility of indicating leakage before failures occur.

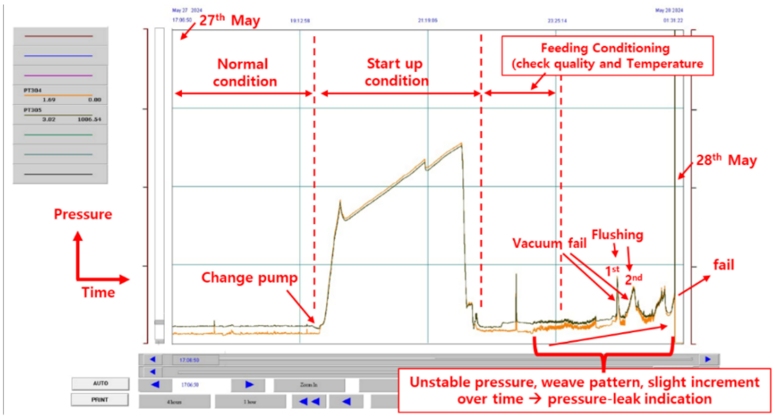

Figure 5.
Pressure Level Monitoring

The samples collected during the site visit were investigated in the laboratory for tensile strength testing, optical emission spectrometers, SEM, and metallographic examination. The metallographic examination starts with sample preparation based on ASTM E3 (American Society for Testing and Materials, 1995). The sample continued to be etched based on ASTM E407 (American Society for Testing and Materials, 2007) to reveal microstructure including grain boundaries.

a. Cross-Sectional Image

To verify the incomplete joint penetration examination on failure area specifically at welding, a microstructural observation has been conducted on the 12 mm/6 mm welded joints. Figure 6 displays the cross-sectional picture of the welded joints that were chosen from the vertical vacuum chamber. The incomplete joint penetration is readily evident and confirms the findings of the visual investigation results during the visit. It is important to note that the weld zone, also known as the fusion zone, is free from any flaws such as porosity, slag inclusion, or any other imperfections. Furthermore, there is no visible trace of the fracture that forms within the heat affected zone (HAZ). Considering the given information, the welding process exhibited satisfactory performance overall, with the exception of inadequate penetration of the welding joint. While the stainless-steel material employed in this vacuum chamber from the condenser to the deodorizer tray is typically resistant to corrosion and still has possibility to be attacked by corrosion, the cross-sectional picture does not show any signs of susceptibility to corrosion. The absence of any pitting on both the welding root and the surfaces of the stainless-steel plates indicates these conditions as shown in Figure 6.

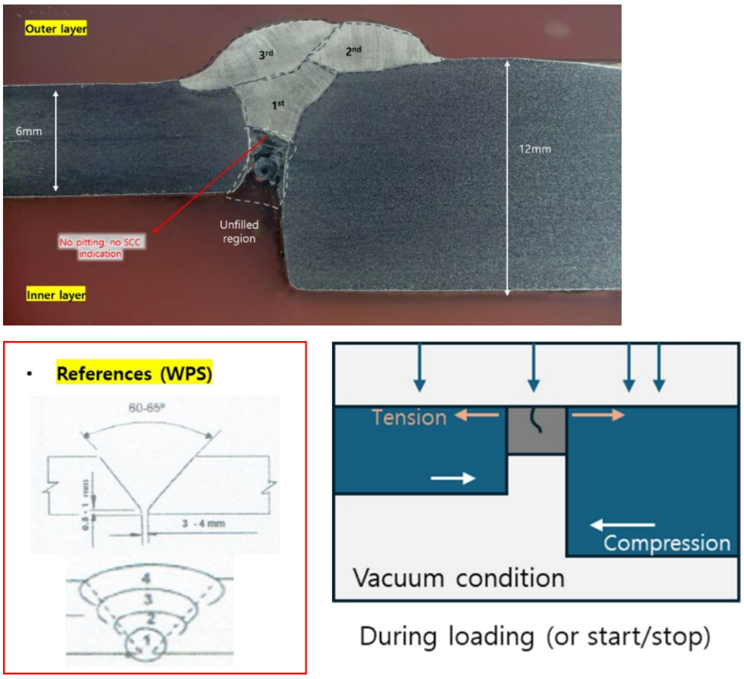

Figure 6.
Cross-Section Image of the Welded Joints

The WPS document states that the welded joint design should be produced using a single-V groove. Regrettably, the cross-sectional image provided indicates that the single-V groove was not adequately prepared prior to the welding procedure. The incomplete joint penetration, as indicated by visual investigation and microstructure observations, suggests that this region may serve as a vulnerable point for stress concentration or potential failure in the overall structure of the condenser-to-deodorizer vacuum chamber. The tension and compression stresses would readily accumulate at the vulnerable point, as seen in Figure 6, during the whole process of production (i.e., mechanical and thermal expansion). Furthermore, it is anticipated that the cracks would persist in this area for an extended duration. As the crack extended and the area decreased (P=F/A), the stress exceeded the strength of the weak point, leading to eventual fracture. Furthermore, the pressure level monitoring detected a leakage signal around one hour before to the ultimate fracture. This proved that the crack had already caused a leakage in the weak spot structure. Within one hour, the weak spot was no longer able to withstand the load.

b. Fracture Surface Observations

Fracture mechanics were used to investigate the fatigue strength of stainless-steel welded joints (Yang Peng, Jie Chen, Jun Dong., 2019), (Razmjoo, G.R., 1995). The observations of the fracture surface may be categorized into two regions: one from the expansion structures and the other from the welded joints. Figure 7. displays the fracture surface of the welded joints that were welded on-site within the vertical vacuum chamber. As expected, the fracture has indeed manifested on the surface of the weld zone, namely at this weak spot. When employing scanning electron microscopy (SEM) at a greater magnification, beach marks have been detected on the fracture surface. According to this evidence, it has been verified that there was fatigue stress cycle present in these welded joints.

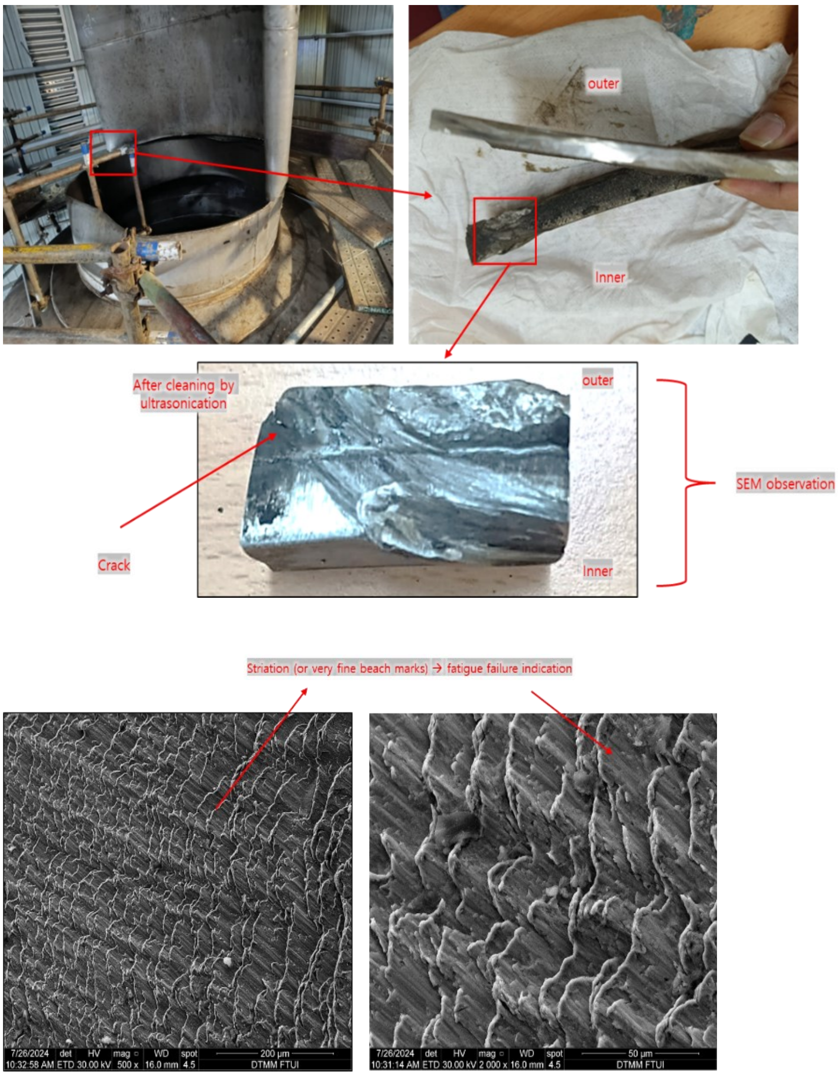

Figure 7.
Fracture Surface of the Welded Joints within the Vertical Vacuum Chamber

On the other hand, Figure 8 displays the fracture surface on the expansion structures. According to the scanning electron microscope (SEM) picture, the fracture surface does not exhibit any beach mark pattern. It suggests that the failure of these expansion structures was not caused by fatigue stress cycle. The presence of dimple patterns on the fracture surface suggests that plastic deformation occurred prior to the failure of these expansion structures. This indicates that the failures in these expansion structures occurred solely under situations of excessive stress or as a consequence of the first failure (i.e. after effect).

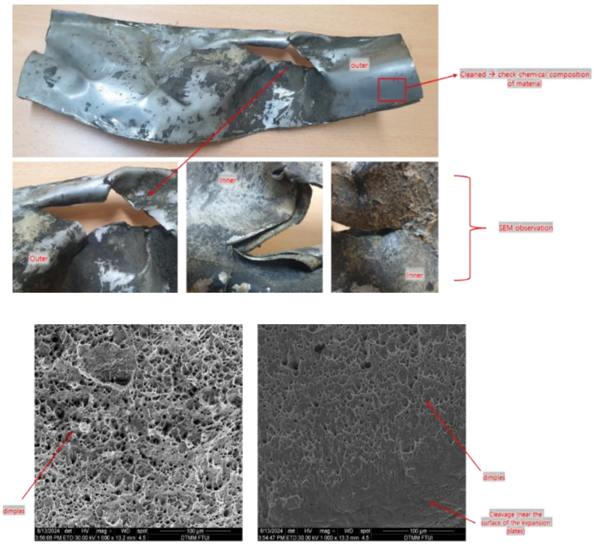

Figure 8.
Fracture Surface of the Welded Joints Expansion Structures

c. Material Specification Conformity

To verify compliance with the specified standards for the expansion structures and vacuum chamber plates, the chemical composition of the materials used (i.e. expansion structure, 6mm chamber plate, and 12 mm chamber plate) was examined using Optical Emission Spectrometer (OES) based on ASTM E1009-95 (American Society for Testing and Materials, 1995). Figure 9 and Figure 10 displays the findings of the chemical composition investigation. Based on the results, it appears that the materials utilized for expansion structures and vacuum chamber plates meet the material specifications for SUS 304 (which mentioned on the WPS document). Moreover, it indicates that there are no issues with the materials aspect.

- Chemical composition examination

	Fe	C	Cr	Ni	Mn	Mo	Co	Si	P	S	Cu	Al
sample 1	Bal.	0.024	18.24	8.306	1.263	0.171	0.067	0.42	0.012	0.0056	0.214	0.0061
sample 2	Bal.	0.021	18.4	8.123	1.691	0.288	0.175	0.338	0.015	0.0032	0.262	0.0063

- References

	Type 304	Type 316
Carbon	0.08% max.	0.08% max.
Manganese	2.00% max.	2.00% max.
Phosphorus	0.045% max.	0.045% max.
Sulfur	0.030% max.	0.030% max.
Silicon	1.00% max.	1.00% max.
Chromium	18.00-20.00	16.00-18.00
Nickel	8.00-10.50%	10.00-14.00

*Mill Certificates are not provided

- According to the references, **there were no signs of any alteration in the chemical composition** of the SUS plates (that installed and welded at Condenser-to-Deodorizer connection line).

Figure 9.
Chemical Composition Investigation for Material Specification of Vacuum Chamber Plates

	Fe	C	Cr	Ni	Mn	Mo	Co	Si	P	S	Cu	Al
expansion joints	Bal.	0.016	18.69	8.155	1.503	0.164	0.209	0.411	0.014	<0.0030	0.131	0.0049

- References

	Type 304	Type 316
Carbon	0.08% max.	0.08% max.
Manganese	2.00% max.	2.00% max.
Phosphorus	0.045% max.	0.045% max.
Sulfur	0.030% max.	0.030% max.
Silicon	1.00% max.	1.00% max.
Chromium	18.00-20.00	16.00-18.00
Nickel	8.00-10.50%	10.00-14.00

*Mill Certificates are not provided

- According to the references, there were no signs of any alteration in the chemical composition of the expansion joints at the horizontal vacuum chamber.

Figure 10.
Chemical Composition Investigation for Material Specification of Expansion Structures

d. Welded Joint Strength Properties Evaluation

To verify the accuracy of the claim that the welding joints being welded on-site have a low mechanical characteristic, tensile testing has been conducted on numerous specimens. Tensile testing was conducted base on ASTM E8 (American Society for Testing and Materials, 2022). Figure 11 displays the tensile characteristics of the welded joints, which were evaluated according to the approval requirements stated in the ASME Sec.IX code. As a rule of thumb for a welding quality, it is essential that the strength of the welded joints surpasses or at least matches that of the underlying material. Unfortunately, the tensile test results for the welded joints revealed values ranging from 245-289 MPa, which significantly deviate from the acceptable criterion specified as 485-515 Mpa (American Society of Mechanical Engineers, 2023).

Tensile Specimen	Joining Strength	
	Kg/mm2	MPa
A	26.62	261.05
B	29.45	288.81
C	25.04	245.56
D	24.94	244.58

- The joining strength: 245-289 MPa,
- Fracture position: welded area

Figure 11.
Tensile Properties (Joining Strength of the Welded Joints)

3. RESULT & DISCUSSION

The first collapse was caused by the failure of the welded joints that were welded on-site. This location is particularly vulnerable to stress concentration and crack formation, making it the weakest point. Subsequently, the failure of the expansion structures (corrugated structure in the horizontal vacuum chamber) might be attributed to the consequences of the first failures.

Due to striation present on weld joint that were welded on-site in the vertical vacuum chamber, the possibility to suspect that the first failure occurred on the expansion structures (or expansion bellows) is invalid despite that the expansion structure have a lower thickness compared to the welded joints that can be suspected for easier stress being concentrated (P=F/A). The pressure level monitoring indicates any leakage or sudden loss of pressure control, and there were no striation patterns on the fracture surface of expansion structure. The evidence suggests that there was a leakage indication for approximately one hour prior to the failure, this indicated the crack from fatigue failure caused the vacuum failure and the vacuum pump still attempt to reach the ideal condition which caused the collapse due to the crack propagated and the remaining area could not withstand the pressure.

If a corrosion attack occurs, the microstructure should quickly identify any indications of corrosion at the failure area in the form of pitting. The evidence revealed the absence of any signs of pitting or other forms of corrosion. Consequently, the minor contaminations resulting from the fatty acid pump failures at the ice condenser-to-deoxidizer connection vacuum chamber do not influence the progression of corrosion product formation. Therefore, final failures exhibit weak connections with the failures of the fatty acid pump. Based on the above failure analyses, this failure was caused by a fatigue mechanism. Fatigue failure occurs due to cyclic loading that is still below the material's yield strength. In this case, cyclic loading resulted from the start and stop processes that occurred several times in the deodorizer. Each time the deodorizer was operated, the stress from thermal stress and pressure changes was responded to by the material as a form of cyclic loading. There are three steps in fatigue failure mechanisms (Figure 12).

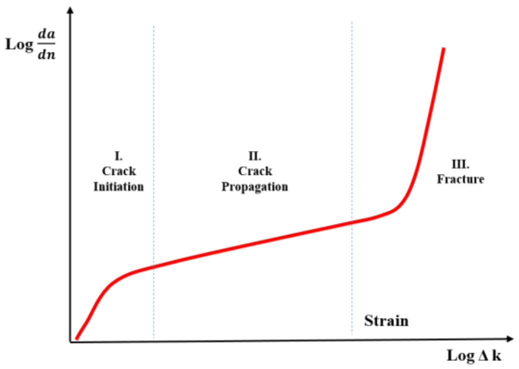

Figure 12.
Graph for Stages of Fatigue failure (Grasp Engineering, 2025)

Stage 1: Crack initiation — Fatigue cracks typically begin at a free surface and near areas of concentrated stress, in this case the defect in welding area. The early stages of fatigue crack formation occur at localized disruptions within the metal's crystal structure. The creation and movement of these disruptions actually reinforce the metal through a process known as work hardening, which involves plastic deformation. As the metal undergoes work hardening, it loses its capacity to plastically deform in the areas subjected to cyclic stresses. When the metal reaches its limit for plastic deformation, these disruptions evolve into small cracks.

Stage 2: Crack propagation — After a crack is initiated, repeated cyclical stresses gradually extend the micro-crack, eventually posing a threat to the structural integrity.

Stage 3: Failure — The final failure event, whether a catastrophic fracture is ductile or brittle, depends on factors such as the material, thickness, temperature, and applied stress. Fatigue failures often happen unexpectedly. The fracture surfaces caused by fatigue in a broken component are usually smooth and show no signs of plastic deformation.

As previously mentioned, the failure that occurred in the vertical vacuum chamber area was more likely due to imperfect welding conditions as a crack initiation, combined with a difference in plate thickness in this section. The most significant welding failure was found in the structure's joint, specifically where the plates of different thicknesses, 12 mm and 6 mm, were connected. After the crack initiated in the imperfect welding joint, it will propagate. The thinner 6 mm plate allows crack propagation to occur more easily in this section.

4. CONCLUSION

There were several events that occurred leading up to or coinciding with the failure of the deodorizer. The events began with a pump failure, which was then repaired, and afterward, the vacuum pressure started to become unstable before eventually leading to the failure incident. After the failure, two areas were investigated for crack, namely the crack on the expansion bellow and crack on the vacuum chamber. Therefore, there are potentially three locations that could have possibility contribution the failure that needed to be examine. To explore the possible causes, the investigation started with the potential contribution of failure due to the crack in the vacuum bellow. The test results for this area suggest that the failure was caused by an overload event, as indicated by the presence of dimple. Since there is no report that showing a sudden overpressure before the incident, the probability for the expansion below failure as the initiation of failure is low.

Another event which suspected to be a contributing cause is the failure of the fatty acid pump, which led to an excess of fatty acid entering the vacuum chamber, potentially causing a corrosion reaction with the structural material. However, this possibility is relatively low as there were no significant signs of corrosion found on the weld tear in the vacuum chamber.

Since both of the possibility mentioned earlier has lower probability as a failure initiation, the most likely primary cause of the failure in this case is the quality of the on-site welded joints, which may have led to the initiation of the failure. These joints serve as the most vulnerable area for stress concentration during the loading and unloading operations of the refinery plant due to improper weld joints resulted with incomplete joint penetration. The loading and unloading operation could make a cyclic thermal stress and cyclic operation pressure. Based on client data, there are several incidents that make the deoxidizer has to stop the operation due to some problem for example pump failure.

This loading and unloading operation could make a fluctuating dynamic stress. In addition to the fluctuating dynamic stresses, there was a high possibility that a crack might developed and gradually propagated in the welded joints, eventually leading to a catastrophic failure. Moreover, the welding joint has been proved have low mechanical properties as shown in tensile test result. In the end, the most possible of failure mechanism observed in these vacuum chambers was fatigue failure. Weld joint play an important role in the manufacture of the engineering components but it usually becomes the weakest point in the whole structures due to the occurrence of the geometrical discontinuity, welding defects and residual stresses, especially under the cyclic loading (Jiang, Wenchun; Xie, Xuefang; Wang, Tianjiao; Zhang, Xiancheng; Tu , Shan-Tung; Wang, Jinguang; Zhao, Xu. (2021).

After crack initiation, the crack will propagate towards the weaker area. In this case, it moved to the 6 mm plate. The thinner section will have a lower capacity to withstand crack propagation since it has a smaller cross-sectional area to distribute the stress.

Based on this root cause analysis, some recommendations are emphasized:

- Follow the welding procedure specification (WPS) document.
- Inspect the preparation of the welding process to ensure that the single-V groove is being prepared appropriately.
- Inspect the weld during and/or after the welding process to ensure that it has achieved complete joint penetration.
- Employ another non-destructive testing method, such as radiography, to verify the completeness of the joint penetration.
- Reduce non planned start and stop / loading and unloading operation which could lead to cyclic stress which trigger the fatigue damage mechanism in the critical part of the equipment.

5. REFERENCES

1. Yang Peng, Jie Chen, Jun Dong. (2019) "Experimental Data Assessment and Fatigue Design Recommendation for Stainless-Steel Welded Joints", *Metals* 9(7): 723. Basel: MDPI.
2. ASME (2023). Boiler and Pressure Vessel Code, Section IX: *Welding, Brazing, and Fusing Qualifications*. ASME BPVC-IX. New York: American Society of Mechanical Engineers.
3. Razmjoo, G.R. (1995). Design Guidance on Fatigue of Welded Stainless Steel Joints. In *Proceedings of the International Conference on Onshore Mechanics and Arctic Engineering*, Copenhagen, Denmark, 18–22 June 1995.
4. Grasp Engineering (2025). *What is Fatigue Analysis? Stages of Fatigue Analysis* (https://www.graspengineering.com/what-is-fatigue-analysis-stages-of-fatigue-analysis/) . Accessed: June 25th, 2025.
5. Jiang, Wenchun; Xie, Xuefang; Wang, Tianjiao; Zhang, Xiancheng; Tu , Shan-Tung; Wang, Jinguang; Zhao, Xu. (2021) "Fatigue life prediction of 316L stainless steel weld joint including the role of residual stress and its evolution", Int. J. Fatigue 143. Qingdao: Elsevier.
6. American Society for Testing and Materials (2022), ASTM E8/E8M*: Standard Test Methods for Tension Testing of Metallic Materials*. West Conshohocken, PA: ASTM International.
7. American Society for Testing and Materials (1995), ASTM E1009-95: Standard Practice for Evaluating an Optical Emission Vacuum Spectrometer to Analyze Carbon and Low-Alloy Steel. West Conshohocken, PA: ASTM International.
8. American Society for Testing and Materials (1995), ASTM E3-95*: Standard Practice for Preparation of Metallographic Specimens*. West Conshohocken, PA: ASTM International.
9. American Society for Testing and Materials (2007), ASTM E407-07*: Standard Practice for Microetching Metals and Alloys*. West Conshohocken, PA: ASTM International.